Comprehensive Laboratory Test Series for Timber-Concrete Composite Structures

Harrach Dániel, Majid Movahedi Rad*

Department of Structural and Geotechnical Engineering, Széchenyi István University, Egyetem tér 1, H-9026 Győr, Hungary
e-mail: harrach.daniel@sze.hu, majidmr@sze.hu

Abstract: Timber-concrete composite structures are not as widespread as traditional steel-concrete fabrications; this structural design still has many critical points that require tests on laboratory specimens. This paper presents the complex testing process of timber-concrete composite structures, which must be followed from the investigation of the possibilities of connecting timber and concrete to each other, through the tests of bended beams acting as timber-concrete composites, to the laboratory tests of full-scale custom-designed timber-concrete composite bridge structures subjected to both concentrated and distributed loads. In this study, to improve the flexural properties of timber beams, carbon fiber-reinforced polymer (CFRP) laminates are attached externally to timber elements. To verify the behavior of the designed structure, we built a full-scale experimental structure and performed a load test. In the laboratory tests, the serviceability limit states, standard loads and load arrangements were investigated. The results of the loading experiments were evaluated. The bridge structures in this article will be placed outdoors after completion of the tests, where they will be used as pedestrian-bicycle bridges. In the case of the examined structures, it was an important aspect, to use elements that are commercially available and suitable for use in the Hungarian design and regulatory systems.

Keywords: — Timber-concrete structures; connections; composite structures; bridge model; static load

1 Introduction

"Composite structures are structures made of several different materials, in which at the moment of assembly, at least one part of the support made of material has considerable stiffness and load capacity. In addition, it is also important that the static characteristics of the structure are calculated according to the rules of elasticity, taking into account changes in stiffness over time.

According to the narrower interpretation, a bent beam or beam grid is called a composites structure, which consists of a steel beam with bending stiffness at the moment of installation, the reinforced concrete slab above it, and sufficiently rigid joint connecting the two structural elements." [1].

Timber-concrete composite (TCC) structures produced using two elements (tensioned wooden beam and compressed reinforced concrete slab) where composite structures can be considered as modern structures [2]. Wood is a natural/renewable building material and reinforced concrete is a modern building material. In this work, the timber beams are located in a protected place under the reinforced concrete slab, which protects the wood from the swelling effects caused by precipitation. [3]

The composite system created from two structure parts with different properties has a significantly higher load capacity and stiffness compared to (purely) wooden structures, and a significantly lower self-weight compared to concrete and reinforced concrete structures. Concrete behaves well against compressive forces, but its tensile strength is low and its self-weight (compared to wood) is significant. Compared to other building materials, wood has a much lower self-weight and a high tensile strength value (the density-strength ratio is very favorable).

In case of outdoor application (e.g.: pedestrian bridge superstructure), an additional advantage is that the concrete layer protects the wooden beams from environmental effects (e.g.: direct rain or sunlight), thus increasing its service life. To use timber and concrete as a composite structure, it is necessary for the elements to work together. Ensuring adequate relationship rigidity is the main goal that is able to transfer shear forces at the connected part of the structure [4] [5]. Figure 1 illustrates the normal stress diagrams that develop depending on the type of connection.

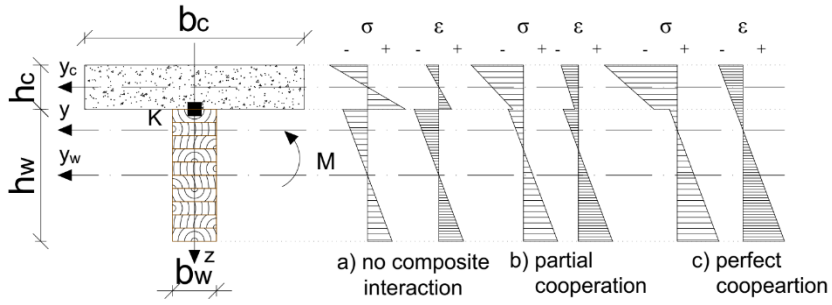

Figure 1

Possible connection levels of timber-concrete structures

The connection stiffness, which can be determined based on the tests, shows the resistance to displacement on the connection surface of the two parts during loading of the structure. K is the connection stiffness, a scalar value that expresses the degree of cooperation between two structural elements. The higher the value, the more cooperation prevails, see Figure 1 [6]:

K<*5.000 N/mm - no composite interaction*

- ***K***=*5-100,000 N/mm - partial cooperation*
- ***K***>*100,000 N/mm - perfect cooperation*

The timber-concrete composite structural system has a history of almost 100 years, the first real-scale experiments on timber-concrete composite beams were conducted between 1938 and 1942, with the aim of comparing the behavior of different connection methods [7].

The analysis of the TCC structures are based on the dimensioning principle of flexibly connected multi-part bent beams, where the entire moment of inertia of the entire cross-section can be calculated, but the deformation of the connecting elements must be taken into account. Most design procedures (e.g. the Eurocode 5's γ-method [8], the stiffness method [9], Girhammar's simplified analysis method [10]) are based on this connection stiffness factor, which must be determined experimentally.

Timber-concrete composite bridges are widespread in the western and northern parts of Europe [5]. In the case of timber bridges with a lifespan of more than 30 years and wooden structures with insufficient load-bearing capacity, the idea to reinforce the wooden beams with a concrete slab first came to light. In the 21st Century, perhaps the most important aspect in bridge construction is no longer applied to meet the requirements of functional needs where the aspects of structure selection do not determine the traffic requirements alone. In addition to load-bearing capacity, durability and economy are the most important design considerations, but aesthetics and environmental awareness have always been important in the design of modern bridges and structures.

In order to achieve an optimal timber-concrete composite behavior, the neutral axis must be located in the vicinity of the contact plane. [11] The stiffness ratio and the strength of the materials show that the ratio of the optimal structural element thickness between timber and concrete should be around 1:10 [12]. However, this ratio is not economical in the case of small bridge structures because the design standards and design regulations prescribe a minimum reinforced concrete slab thickness of 15-20 cm depending on the structural variation in e-UT 07.01.14:2011 [13].

In this paper, we deal with the process from the measurements of the connection between timber and concrete to the static load test of the full-scale (6.0 m span, 2.4 m wide) bridge model in laboratory conditions. The special feature of the designed TCC bridges, that they have been designed in such a way that they can be used as an actual pedestrian-bicycle bridge with minimal reconstruction. During the design of the experimental program, it was important to match the bridge structures to the real traffic loads.

2 Connecting Timber and Concrete

In order to determine the mechanical properties of any composite structure, it is essential to know the strength and deformation characteristics of the joint that connects the different materials. In the case of a timber-concrete composite system, these are influenced by the type of connection. When considering the characteristics of wood and concrete, the initial slip between the two support sections and the effective bending stiffness of the composite system are taken into consideration.

However, it is important to note that joining timber and concrete does not mean joining two perfectly rigid materials. For the Timber-concrete composite (TCC) connection, the difference is that of the steel-concrete composite, so that the coupling element can be moved, pivoted and pushed in both the wood and the concrete [14]. Both wood and concrete have time-dependent properties (shrinkage, swelling, permanent deformation), in the case of design an optimal connection, the coupling element must also be able to absorb the resulting additional stresses [6].

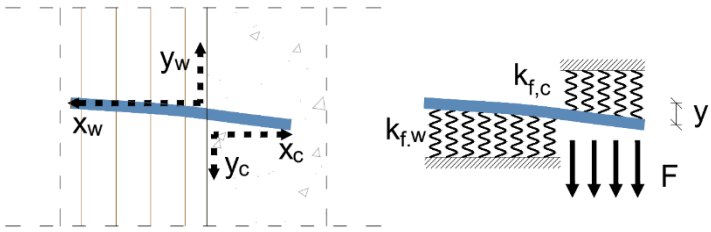

Figure 2
The model of the connection of timber-concrete composite structures [4]

When designing the connections of timber-concrete composite structures, the linear-elastic connection stiffness models only give appreciable results in a very narrow range. The dimensioning procedure that takes into account the non-linear behaviours of the connection exists only at a theoretical level and cannot currently be used for calculations. Its essence is that in the case of relationships and material properties, it calls for a transition from Hooke's linear material model and Winkler's spring model to higher-level theories and functions [14].

The mechanical properties of the connection influence the behaviour of the structure (distribution of stresses, deformations). The classification of shear connections was carried out by Ceccotti [4], who classified the connections, based on their stiffness.

Class A: Inexpensive, easy-to-build, low-rigidity connections

Class B: Connections with greater stiffness and ductility

Class C: Shear wedges reinforced with anchoring units

Class D: Connections with the greatest stiffness. There is no slippage between the two structural elements

2.1 Test Method for the Connection between Timber and Concrete

To test the connection between wood and concrete, researchers typically follow the requirements of the EN 26891:1997 [15] and ASTM D5652-21 [16] and EN 1994-1-1:2010 [17] and based on this, they develop their experimental method for examining wood-concrete composite connections. Three different layouts are used for shear testing of wood-concrete composite structures: Pure shear test specimen, Single shear push out test specimen and Double shear push out test specimen. There are two types of the last, when the wood is surrounded between two sides of concrete (CWC concrete-wood-concrete), and when the concrete is located between two wooden parts (WCW wood-concrete-wood). Figure 3 shows the test arrangements for the connection between wood and concrete.

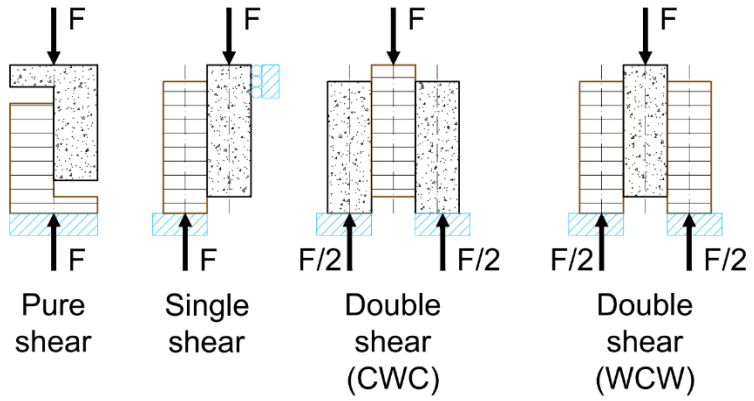

Figure 3
The most common wood-concrete connection test assemblies [18]

2.2 Push-Out Tests

When choosing the test method, I took into account the recommendations of Ceccotti [4] and Holschemacher et al [19], and to determine the connection stiffness, twice sheared push-out wood-concrete-wood (WCW) test specimens I made. The test specimens were designed uniformly with a contact surface of 100x200 mm, because the smaller test specimens can be produced in large quantities and in good quality. The geometry of the test specimens is a 150x100x250 mm wooden beam and a 130x100x250 mm concrete beam adapted to the type of connecting element. A total of 10 different types of connection designs were made, three test specimens per connection type. The characteristics of the test specimens are listed in Table 1.

Table 1
The main characteristics of test specimens for the connection between wood and concrete

Type	*Connection method*	*Contact element quantity*
ACS	threaded rod with a tightening torque of 109 Nm	1 pc M20-8.8 – Ø20
ICO	flexible adhesive	Icosit® KC 340/65
RM	epoxy adhesive	Sikadur®-31 CF Normal
FCS90	timber-concrete screw at 90°	1 pc VB-48-7,5x100
FCS45	timber-concrete screw at 45°	1 pc VB-48-7,5x100
FCS±45	timber-concrete screw at ±45°	2 pc VB-48-7,5x100
BB45	bent rebar	1 pc B500B - Ø8 Sikadur®-30 Normal
EA	glued perforated steel plate	1 pc 120x200x3mm Stw. 22, stainless steel Sikadur®–52 Injection Normal
KFCS	glued hardwood dowel	1 pc hardwood dowel: D24 (Ø20) Sikadur®-30 Normal
ICOPL	flexibly embedded perforated steel sheet	1 pc 120x200x3mm Stw. 22, glued hardwood dowel Icosit® KC 340/65

The concrete part is made with non-reinforced construction, uniformly with concrete quality C35/45-XA1-XC4-XD3-XF2-16-F3, while the timber's material quality C24. Figure 4 show the design of the connection test specimens. The tests were perforated based on the loading procedure of the MSZ EN 26891:1995 [15] standard.

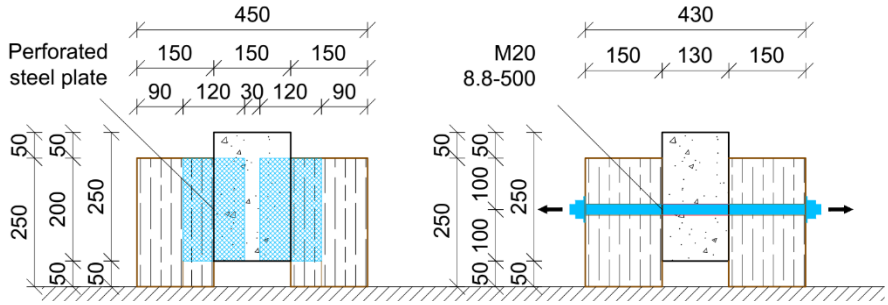

Figure 4
The plans of the test specimens EA and ACS

2.3 Test Results

The main test results are contained in Table 2. The connection stiffness values to be used during linear design methods, i.e. the connection stiffness value for the service

limit state ***(K_{ser})*** and the ultimate limit state (***K_u***). In addition, the ***K(x)*** function of stiffness for the implementation of non-linear design methods was given.

Table 2
The main results of push-out tests

Type	F_{max} [kN]	K_{ser} [kN/mm]	K_u [kN/mm]	***K(x)*** **Function of the connection stiffness**
ACS	94.9	38.5	23.8	$K(x)$= if x≤0.2 → 221.97x if x>0.2 → 4.8145x+43.431
ICO	119.4	42.5	32.5	$K(x) = -3.2333x^2 + 40.021x$
RM	125.4	170.0	194.3	$K(x) = 174.76x^{0.8013}$
FCS90	25.8	3.9	2.3	$K(x) = -0.0765x^2 + 2.8122x$
FCS45	10.0	8.7	7.8	$K(x) = 1.1342\ln(x) + 6.8077$
FCS±45	56.3	193.5	121.3	$K(x) = 7.2937\ln(x) + 39.11$
BB45	20.6	41.0	28.2	$K(x) = 1.8245\ln(x) + 13.32$
EA	83.2	73.8	70.0	$K(x) = -9.8284x^2 + 63.371x$
KFCS	36.2	11.0	5.8	$K(x) = -4.7948\ln(x) + 15.412$
ICOPL	56.2	59.0	35.1	$K(x) = 6.2976\ln(x) + 31.573$

The connection type with sufficient connection stiffness and ductile reserve -out of the 10 different connection designs examined - is the shear connection with perforated steel plate glued into the timber part (EA) when using a monolithic reinforced concrete. While using a prefabricated reinforced concrete, the threaded rods (ACS) gives favorable design. Figure 5 shows the typical force-displacement diagram of the various connection types measured during the experiment.

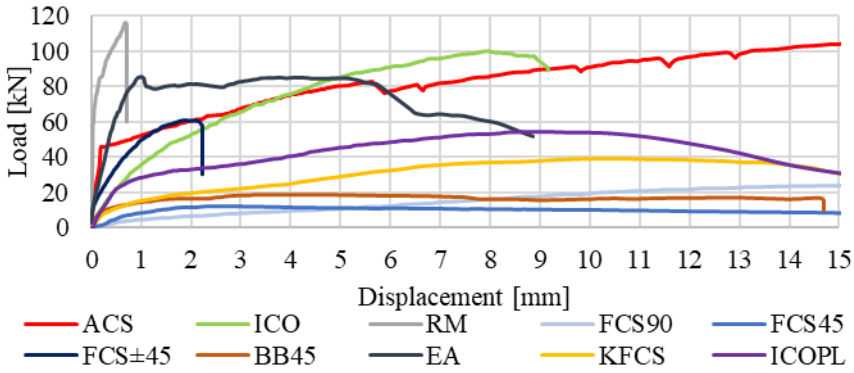

Figure 5
Characteristic force-displacement diagrams

3 Timber-Concrete Composite Beams

Timber-concrete composite structures are most often used as two-support, bent beams. The timber-concrete composite bridges built in Europe were used almost exclusively as simply supported, upper-track beams.

Accordingly, the laboratory measurements of TCC were carried out in all cases by examining the three- or four-point bending of simply supported beams, as was done, for example, by Brazilian researchers in [20], Gutkowski's research team [11], and by the Spanish researchers [12] also. During the tests, experiments were carried out in accordance with the principles of EN 408:2010+A1:2012 [21].

In order to reduce the structural height, the timber beams are provided with carbon fiber reinforcement at the tensioned side and as a result, the beam's height can be significantly reduced [22].

3.1 Test Specimens

During the laboratory test, two series of test specimens were loaded. The test specimens were uniformly made of 360x80 mm C35/45 quality reinforced concrete slab (B500B reinforcing steel), 120x240 mm GL24h quality glue laminated timber beams, and two pieces of Sika CarboDur-S-512 lamellas glued to the lower plane of the timber beams with SikaDur-30. The difference between the two series is the different connection system between the two main elements: for the prefabricated reinforced concrete slab: threaded rods with a tightening torque (**ACS)**; for the monolithic reinforced concrete slab: glued perforated steel plate (**EA**) were used.

Table 3
Material parameters for timber-concrete composite beams

	f_c [N/mm^2]	f_t [N/mm^2]	f_v [N/mm^2]	E [kN/mm^2]	ε [N/mm^2]
Concrete	35	3.2		34	0.35
Reinforcement	-	563	-	200	10
CFRP	-	3.100	-	170	1.70
Epoxy	85-95	26-31	16-19	11.2	-
Perforated steel plate	-	510-680		210	-
Injection material	52	37	-	1.8	-

Through Threaded Rods with Friction Connection (1-3)

The threaded rods were M10, material quality 8.8, and were placed in the Ø14 mm sleeves formed in the test specimens. The threaded rods were uniformly tightened with a tightening torque of 49 Nm, thus creating a frictional connection.

Glued Perforated Steel Plate Connection (I-III)

The connection between the concrete and the wooden part is provided by a Qg10-15x3 type Qg10-15x3 square mesh perforated stainless steel plate with a thickness of 3 mm glued to the timber beam with SikaDur-52 Injection.

The cross-sections of the specimens are showed in Figure 6.

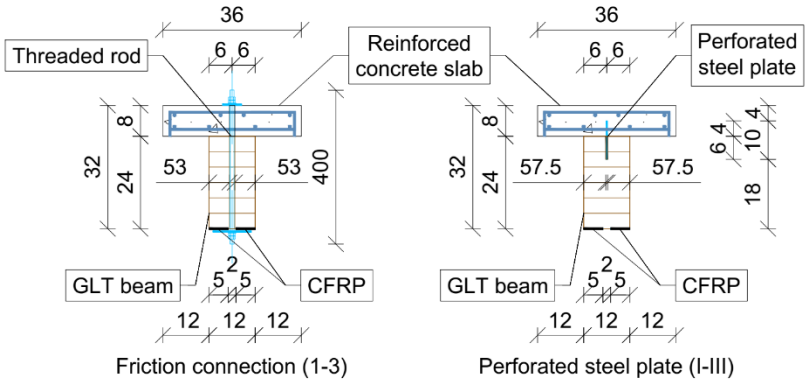

Figure 6
Cross-section of the test specimens (Dimension in cm)

3.2 Test Results

During the tests, three-point loading was carried out, and deformations were measured in three cross-sections (at the center of the support and at the quartering points). At both ends of the beams, fork-shaped, hinged supports were placed. Furthermore, the end plate displacement between the timber and concrete part was examined, with the test layout as can be seen at Figure 7.

Figure 7
The test layout of the three-point bending test of timber-concrete composite beams

Figure 8 shows the deflection of the central cross section of the composite beams during the loading process. On the diagram, I also marked the theoretical deflection function of the timber beam, and the different connection levels "Perfect" and "Partial" based on EN 1995-1-1:2010 [8].

In the case of a frictional connection, based on the measurement of the slippage between the timber and concrete part, no displacement occurs up to a load value of ~30-35 kN, the friction holds the two parts together, but after that the two parts slide in relation to each other. This slippage is permanent, i.e. the two support parts did not return to their original position during or at the end of the load cycles.

The failure of the beams was caused by the fact that the threaded rods were no longer able to prevent the sliding of the timber and concrete elements beyond the friction limit.

In the case of the perforated plate connection, based on the slippage between the wooden and concrete parts, the stiffness of the connection is constant up to a load value of ~60 kN, but after that the behaviour of the connection is no longer linear.

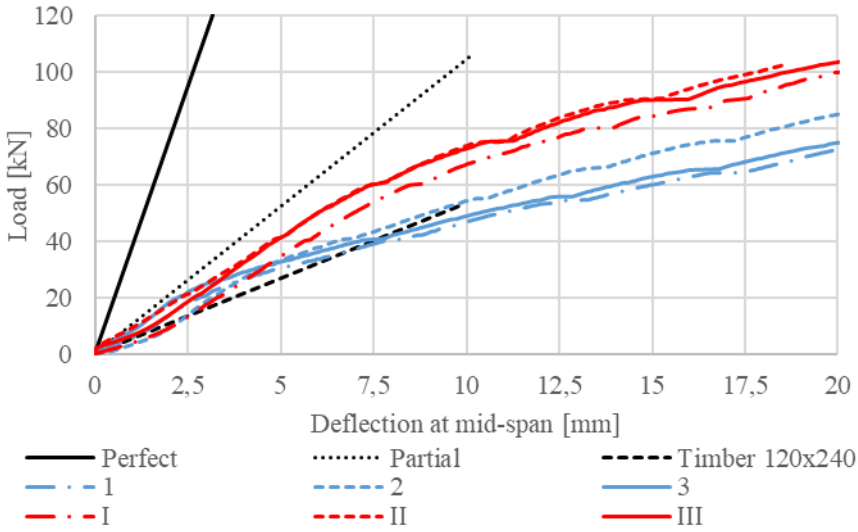

Figure 8

Deflection of the central cross-section as a function of the load force

In the case of the perforated plate specimens, the failure was caused by the fact that the glued-laminated beams were not able to withstand the stresses resulting from bending. The plane of failure occurred above the lower lamella of the laminated glued support, the two lower lamellas were sheared due to horizontal sliding forces, as shown in Figure 9.

Figure 9
Shearing of the last lamella layer

EN 1995-1-1:2010 [8] works with an excessively large error in the cases we examined, as shown in Table 4, the difference in stiffness is almost double - to the detriment of safety. In addition to the fictitious stiffness values ($\boldsymbol{EI_{fikt}}$), the table below also includes the deflection ($\boldsymbol{e_{30kN}}$) and the breaking load ($\boldsymbol{F_{max}}$) corresponding to a load value of 30 kN.

Table 4
Comparison of measured and calculated test results

	"Perfect"	Perforated steel plate		Frictional connection		*Timber*
	EC5B	EC5B	**TEST**	EC5B	**TEST**	EC5
e_{30kN} [mm]	0.62	1.78	**3.52**	2.01	**3.96**	5.08
F_{max} [kN]	176.13	116.80	**105.04**	109.58	**85.49**	52.66

It can also be seen from the results presented in the table that the results measured under laboratory conditions and those determined by Eurocode calculations working with the simplified linear elastic theory are not even close to the same. The linearly flexible dimensioning according to Eurocode – in comparison with the experimental results – increases the stiffness, deflection by about twice as much, and the breaking strength by approx. It approximates by 10-30% to the detriment of safety. The main reason for this is the neglect of approximations and material/relational nonlinearities in theoretical calculations.

4 Timber-Concrete Composite Bridge Models

4.1 Models

Two timber-concrete composite (TCC) bridges were made with dimensions of 6.5 m bridge length, 6.0 m span, and 2.4 m track width (without parapet). The first bridge has two glue-laminated timber (GLT) girders design (TC-A), while the second has six GLT girders (TC-B). The shear connection between the timber and the concrete is given by a perforated steel plate connection glued into the timber beams along its entire length and the shear elements were connected to the reinforcement of the reinforced concrete traffic deck. The ends of the timber girders are also connected to the cross girder with the same connection type.

Since the case of a connection between concrete and timber, the wood extracts water from the concrete and reduces the strength of the concrete near the connection, a separation layer was built between the timber and the concrete parts in order to separate the water from the wood during the setting of the concrete. The tensioned side of the timber beams was reinforced with CFRP strips to reduce the required structural height of the bridge models. Table 5 provides the properties of the materials used.

Table 5
Materials properties

Material		***Compression strength*** f_c ***[N/mm²]***	***Tensile strength*** f_t ***[N/mm²]***	***Modulus of elasticity*** E ***[N/mm²]***
Concrete	C35/45	35	3.20	34 000
Rebar	B500B	500	500	200 000
CFRP	CarboDur S-1214	-	3.1000	170 000
Epoxy glue	SikaDur 30	-	26-30	11 200
Perforated steel	Qg 10-15-3 S355J	85-95	510-680	210 000
Injection	SikaDur-52	52	37	1 800

Figure 10, displays the cross-section of the TC-A bridge model which has a 12 cm reinforced concrete desk, and two GLT beams - 16x32 cm, also, two shear connections were placed between the timber beam and the reinforced concrete slab.

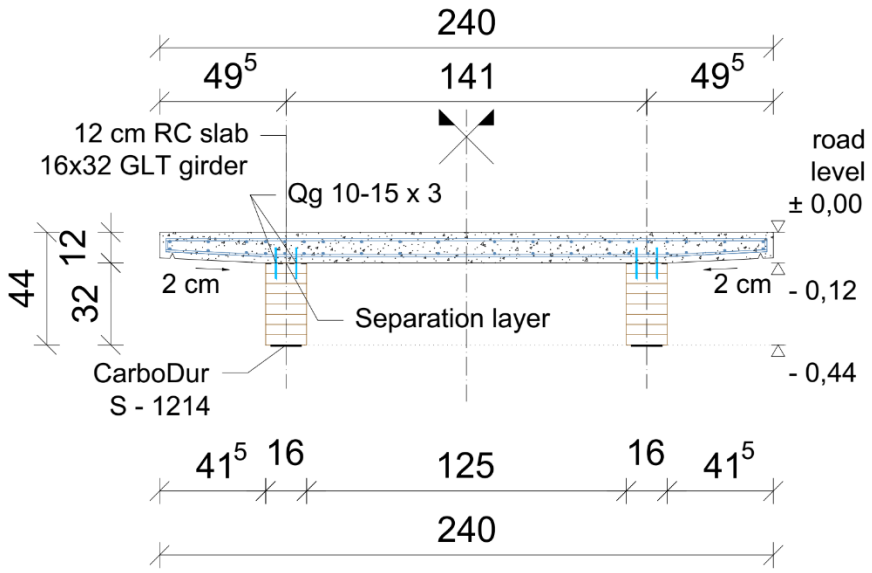

Figure 10
Cross-section of the two girders bridge model (TC-A)

In the case of the six-girders design (TC-B), the thickness of the deck is 8 cm, the timber beams are made with a 12x24 cm cross-sections as shown in Figure 11.

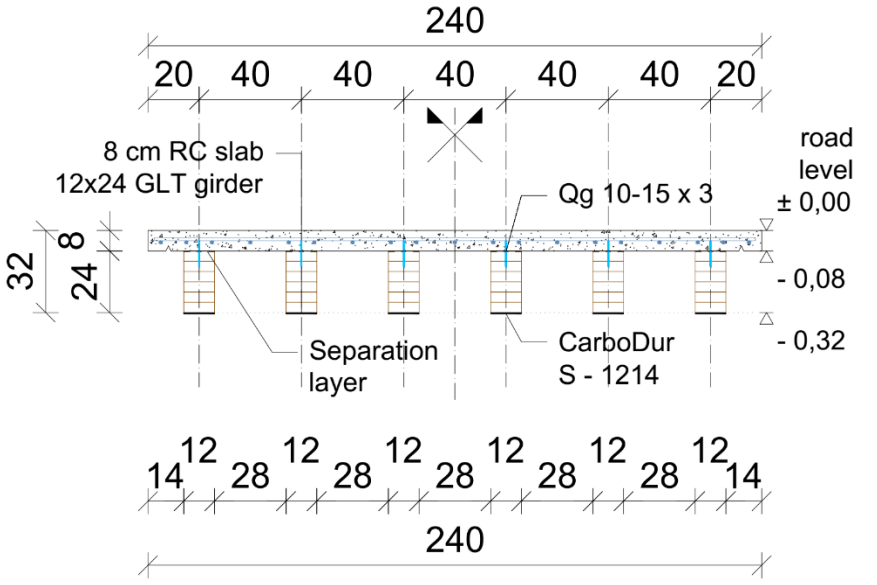

Figure 11
Cross-section of the six girders bridge model (TC-B)

4.2 Loading Process

Several loads were applied to the bridge models in order to simulate the actual behavior. However, the load-bearing limit of the structures could not be reached and the bridges did not load up to failure as the investigation was in operating condition. During the loading process, we followed the regulations of EN 1995-2:2014 [23] and e-UT 07.01.14:2011 [13] standards where the aim was to prove the resistance for the standard loads. The bridge models will be installed in an external site after the laboratory test period as these bridges will be pedestrian-bicycle bridges and according to the planned location, we dealt with the load required for pedestrian-bicycle bridges according to EN 1991-2:2006 [24]

- Distributed load: Load Model No. 1:

  Recommended characteristic value for pedestrian traffic areas and bicycle lanes of short or medium-length footbridges:

  $q_{fk} = 5{,}00\ kN/m^2$ (1)

- Concentrated load: Load Model No. 2:

  To test the local effects, a vertical force shall be applied to a surface of 0.1 x 0.1 m:

  $Q_{f,wk} = 10\ kN$ (2)

- Service Vehicle Load: Load Model No. 3:

  Figure 12 shows the standard load arrangement of the service vehicle according to EC. The arrow indicates the direction of travel of the vehicle.

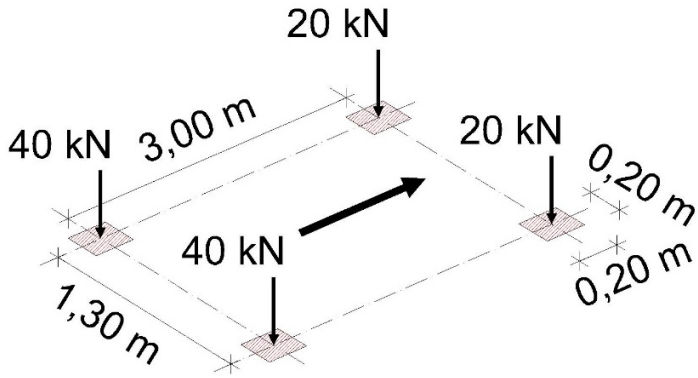

Figure 12
Vertical load model of the service vehicle

Concerning the case of distributed load at an area, different load arrangements have been investigated:

- Full loading (Full)
- Full loading over half the length (Uni)

- One-sided full loading (Lane)
- Checkerboard loading (Chess)

The distributed loading was applied by placing sandbags at the loading area considering load steps of 100 kg/m^2 (1,00 kN/m^2). Figures 13 and 14 shows typical arrangements for the distributed loads.

Figures 13-14
Load arrangements for distributed load (Chess_1 and Lane_1)

In the case of concentrated forces, the following types were examined separately:

- The total load of the service vehicle at the point of maximum bending stress
- The load on the one-sided wheels of the service vehicle at the point of maximum bending stress, placed on the edge of the console
- The load on the main axle of the service vehicle at the middle of the span
- Load of one-sided wheel of the main axle of the service vehicle in the middle of the span, placed on the edge of the console

Figures 15-16
Axle load arrangements during concentrated load (S_1 and A-4)

Axle and wheel loads were tested with forces acting on standard surfaces. Figures 15 and 16 shows the test setups of the concentrated loading period of the models.

4.3 Test Results

During the load tests, the deflections resulting from the self-weight of the bridges were not measured separately, only the deflections due to overload were recorded. The vertical deflection of the bridges was measured in three different cross-sections at a total of fifteen measuring points during the whole loading process. The load-displacement diagrams obtained during loading showed linear behavior for all measurement points. Besides, the magnitudes of the largest deflection values correspond to the results obtained during the modeling. Figures 17 and 18 shows the shape of the structure as the maximum load value was reached in different representations.

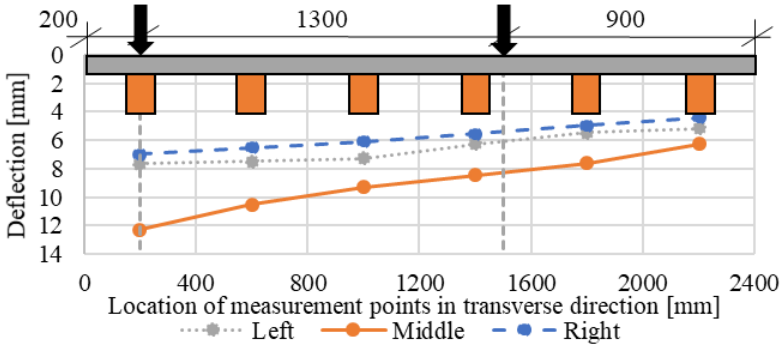

Figure 17
Deflection diagram of the TC-B bridge model under the effect of the total load of the service vehicle in nonsymmetrical arrangements (S_3)

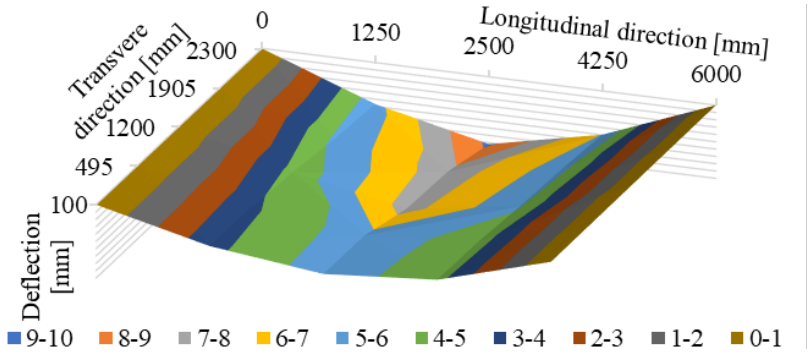

Figure 18
Contour line map of the TC-A bridge model under right-hand eccentric loading at the middle of the bridge (A_2)

Table 6 shows the maximum measured deflection values for TC-A and TC-B bridges under different concentrated loads. The load A_1 to A_4 refers to the asymmetrical load positioning along the bridge model length, the load types S_1 to S_4 refers to the symmetrical concentrated load arrangement.

Table 6
Experimental test results for concentrated load

Load type	*Load location d_x [mm]*	*Eccentricity of load d_y [mm]*	*Load F_{max} [kN]*	*Deflection e_{max} [mm]*	
				TC-A	**TC-B**
A_1	2500	0	2x60 kN	**7.78**	**9.66**
A_2	2500	+350	2x60 kN	**9.21**	**11.54**
A_3	2500	-350	2x60 kN	**8.56**	**12.29**
A_4	2500	-1000	1x60kN	**5.62**	**8.67**
S_1	3000	0	2x40 kN	**5.12**	**6.62**
S_2	3000	+350	2x40 kN	**6.11**	**8.25**
S_3	3000	-350	2x40 kN	**5.90**	**8.01**
S_4	3000	-1000	1x40kN	**3.84**	**5.88**

Table 7 shows the maximum measured deflection values for TC-A and TC-B bridges under different distributed loads. An indexed load of "_2" means an inverse arrangement of an indexed load of "_1".

Table 7
Experimental test results for distributed loads

Load type	*Load q_{max} [kN/m^2]*	*Deflection e_{max} [mm]*	
		TC-A	**TC-B**
Full	5.00	**3.21**	**3.54**
Chess_1	5.00	**1.75**	**1.89**
Chess_2	5.00	**1.74**	**1.90**
Uni_1	5.00	**1.61**	**1.89**
Uni_2	5.00	**1.65**	**1.97**
Lane_1	5.00	**1.96**	**2.78**
Lane_2	5.00	**1.91**	**2.64**

Based on the results of the tests, both bridge structures remained in the operating load level due to the load as no permanent deformations have occurred. Most importantly, it was possible to compare the maximum deflection values by the standards e-UT 07.01.12:2011 [25] and EN 1995:2:2014 [23] prescribes the limit for the maximum deflection of footbridges due to traffic loads as follows:

$$L/400 = \mathbf{15.625}\ mm > e_{max} \tag{3}$$

Conclusion

This paper presents the tests of wood-concrete composite structures under laboratory conditions.

Small-scale push-out tests of the connections between wood and concrete were carried out in order to find the optimal connection system. For the connection to precast concrete, we considered a prestressed, frictional connection to be the best.

Until the friction caused by the tension force ceases, the connection between the two elements can be taken into account with a high value. The wood is loaded perpendicular to the grain direction, by the tension force. This type of connection system requires subsequent maintenance; the planned tension force must be checked during the operating period.

In the case of the connection to monolithic concrete, the perforated plate connection gave the best results, in terms of the stiffness and ductility of the connection. By connecting the steel plate and the reinforcing bars of the reinforced concrete structures, the problem of concrete splitting can also be treated.

A three-point bending test was performed on the composite beams. Using the results of the connection test specimens, we loaded the beams formed with the ACS and EA connection types. As expected, the two connection designs behaved almost identically in the initial (low load) range. During higher loads, however, in the case of the screw connection, the connecting force disappeared and the two structural parts separated from each other.

In the case of timber-concrete beams, the failure was caused by tensile stresses arising from bending on the stretched side of the wood due to the sizes available on the market and required by the construction rules.

The last tests were static trials of timber-concrete composite models, where the behavior of two and six, main girder structures, under concentrated and distributed loads, was examined.

The main aim of this research was to investigate the bridge models under standard loads. After the investigation, the models will become functional bridges, at an external site. Under the bridge standard loads, the structures were adequate, after conversion to road regulations (placing pedestrian parapets, application of the anti-slip coatings…), are suitable to prove against actual traffic. The bridges will be equipped with a monitoring system at the actual installation site, that will provide an opportunity to compare laboratory tests and on-site results, thus, describing the behavior of the structures, as accurately and completely as possible.

References

[1] KISS, L. (2012) „Hídépítés 5.” [Online] Available: https://docplayer.hu/12052901-5-eload-szlo-2012.html

[2] FRAGIACOMO, M, (2012) „Experimental behaviour of a full-scale timber-concrete composite floor with mechanical connectors”, Materials and Structures, Vol. 45, No. 11, pp. 1717-1735, doi: http://dx.doi.org/10.1617/s11527-012-9869-3

[3] BAJZECEROVÁ, V & KANÓCZ, J, (2016) „The Effect of Environment on Timber-concrete Composite Bridge Deck”, Procedia Engineering, Vol. 156, pp. 32-39, doi: http://dx.doi.org/10.1016/j.proeng.2016.08.264

[4] CECCOTTI, A., (1995) „Timber-concrete composite structures". Timber Engineering-STEP 2, Ed. by H. J. Blass, P. Aune, B. S. Choo, R. Görlacher, D. R. Griffiths, B. O. Hilson et al. Centrum Hout, The Netherlands. ISBN 90-5645-002-6

[5] RODRIGUES, JN, DIAS, AMPG & PROVIDÊNCIA, P., (2013) „Timber-Concrete Composite Bridges: State-of-the-Art Review", BioResources, Vol. 8, No. 4, doi: http://dx.doi.org/10.15376/biores.8.4.6630-6649

[6] DIAS A. M. P. G., (2005) „Mechanical behavior of timber-concrete joints", PhD Thesis, University Coimbra, Portugal. ISBN 90-9019214-X

[7] COSTA, L., (2011) „Timber concrete composite floors with prefabricated fibre reinforced concrete", Lund Institute of Technology, ISSN: 0349-4969

[8] EN 1995-1-1:2010: Eurocode 5: Design of timber structures - Part 1-1: General - Common rules and rules for buildings

[9] CVETKOVIC, R & STOJIC, D, (2003) „Design methods of a timber-concrete T-cross-section", Facta universitatis - series: Architecture and Civil Engineering, Vol. 2, No. 5, pp. 329-338, doi: http://dx.doi.org/10.2298/fuace0305329c

[10] GIRHAMMAR, UA, (2009) „A simplified analysis method for composite beams with interlayer slip", International Journal of Mechanical Sciences, Vol. 51, No. 7, pp. 515-530, doi: http://dx.doi.org/10.1016/j.ijmecsci.2009.05.003

[11] GUTKOWSKI, R, BROWN, K, SHIGIDI, A & NATTERER, J, (2008) „Laboratory tests of composite wood–concrete beams", Construction and Building Materials, Vol. 22, No. 6, pp. 1059-1066, doi: http://dx.doi.org/10.1016/j.conbuildmat.2007.03.013

[12] NEGRÃO, JHJ DE O, MAIA DE OLIVEIRA, FM, LEITÃO DE OLIVEIRA, CA & CACHIM, PB, (2010) „Glued Composite Timber-Concrete Beams.II: Analysis and Tests of Beam Specimens", Journal of Structural Engineering, Vol. 136, No. 10, pp. 1246-1254, doi: http://dx.doi.org/10.1061/(asce)st.1943-541x.0000251

[13] e-UT 07.01.14:2011: Beton, vasbeton és feszített vasbeton hidak. Közúti hidak tervezése (KHT) 4

[14] AUCLAIR, SC, SORELLI, L & SALENIKOVICH, A, (2016) „Simplified nonlinear model for timber-concrete composite beams", International Journal of Mechanical Sciences, Vol. 117, pp. 30-42, doi: http://dx.doi.org/10.1016/j.ijmecsci.2016.07.019

[15] EN 26891:1997: Timber structures - Joints made with mechanical fasteners - General principles for the determination of strength and deformation characteristics (ISO 6891:1983)

[16] ASTM D5652-21: Standard Test Methods for Single-Bolt Connections in Wood and Wood-Based Products

[17] EN 1994-1-1:2010: Eurocode 4: Design of composite steel and concrete structures - Part 1-1: General rules and rules for buildings

[18] DIAS, A. M. P. G., MONTEIRO, S. R. S., MARTINS, A. G. D, (2013) „Summary of shear connector methods for timber-concrete composites", Proceedings on Innovative Timber Composites: Improving wood with other materials, Nicosia, Cyp., 17. October 2013. pp. 15-17, ISBN 1 85790 178 9

[19] HOLSCHEMACHER, K., KLOTZ, S., WEISSE, D., (2002) „Application of steel fibre reinforced concrete for timber-concrete composite constructions", Leipzig Annual Civil Engineering Report, University of Leipzig, Germany, Lacer No. 7, 2002, pp. 161-170

[20] MIOTTO, JL & DIAS, AA, (2015) „Structural efficiency of full-scale timber–concrete composite beams strengthened with fiberglass reinforced polymer", Composite Structures, Vol. 128, pp. 145-154, doi: http://dx.doi.org/10.1016/j.compstruct.2015.03.054

[21] EN 408:2010+A1:2012: Timber structures - Structural timber and glued laminated timber - Determination of some physical and mechanical properties

[22] KIM, YJ & HARRIES, KA, (2010) „Modeling of timber beams strengthened with various CFRP composites", Engineering Structures, Vol. 32, No. 10, pp. 3225-3234, doi: http://dx.doi.org/10.1016/j.engstruct.2010.06.011

[23] EN 1995-2:2014: Eurocode 5: Design of timber structures - Part 2: Bridges

[24] EN 1991-2:2006: Eurocode 1: Actions on structures - Part 2: Traffic loads on bridges

[25] e-UT 07.01.12:2011: Erőtani számítás. Közúti hidak tervezése (KHT) 2